Master Thesis: Climate change economic effect on health through temperature

Paulo Gugelmo Cavalheiro Dias

May 16, 2025

Contents

1 Introduction

Temperature is a fundamental component of the physical environment, shaping human activity across multiple dimensions. As climate change alters the global distribution of temperature, there is growing concern about its broader economic consequences. While substantial attention has been given to the direct effects of temperature on labor productivity, agricultural yields, and conflict, less is understood about how temperature-driven changes in health may propagate through the economy over the long run.

Health is a critical input into individual well-being and economic performance. Variations in temperature can influence the incidence and severity of disease, the functioning of the human body, and the demand for medical services. These effects, in turn, may alter labor supply, human capital accumulation, and lifetime income trajectories. Understanding the economic cost associated with these health effects is essential for quantifying the full burden of climate change and for informing effective adaptation policy.

1.1 Related literature

This paper contributes to three main strands of literature: health economics, the economics of climate change, and the intersection of climate and health. Each of these fields provides foundational insights but leaves open important questions regarding the long-run economic consequences of temperature-induced health variation.

1.1.1 Health Economics

A large literature has documented the central role of health in shaping economic behavior over the life cycle. De Nardi et al. (2023) demonstrate that health status significantly affects labor supply, retirement decisions, and savings dynamics, establishing health as a key determinant of productivity and economic welfare. Beyond contemporaneous productivity effects, poor health imposes substantial intertemporal costs. Both De Nardi et al. (2023) and Capatina (2015) quantify the lifetime income and utility losses associated with adverse health trajectories, emphasizing the compounding nature of health shocks over the life course.

1.1.2 Climate and Economics

The economic impacts of climate change are multifaceted, with temperature emerging as a particularly influential channel. Burke et al. (2015) document substantial aggregate output losses associated with rising temperatures, particularly in countries with limited adaptive capacity. More recently, Bilal and Kanzig (2024, 2025) show that temperature shocks have asset-pricing implications, underscoring the forward-looking nature of climate risks.

At the same time, the literature has explored how extreme heat may exacerbate social and political instability. Burke, Hsiang, and Miguel (2015) provide

compelling evidence that hotter temperatures increase the likelihood of conflict in developing countries, suggesting that the consequences of climate change extend well beyond output measures. Importantly, adaptation has been shown to significantly mitigate the economic burden of climate shocks. Carleton et al. (2022) estimate the global mortality consequences of warming while explicitly accounting for adaptation costs and benefits, illustrating how policy and behavioral responses shape climate damages.

From a methodological standpoint, the empirical identification of climate impacts presents persistent challenges. Deryugina and Hsiang (2017), Hsiang (2016), and Nordhaus (2019) all highlight the difficulties of isolating causal effects in the presence of spatial and temporal heterogeneity. Bilal and Kanzig (2024, 2025) further emphasize the econometric complexity involved in measuring forward-looking responses to climate risks.

1.1.3 Climate and Health

A growing body of work links temperature variation to health outcomes. Barreca et al. (2016) show that the temperature-mortality relationship in the U.S. has declined substantially over the twentieth century, pointing to significant adaptation in developed economies. Nevertheless, the potential for major health shocks remains. The IPCC (2022, Chapter 7) outlines the anticipated health risks under various warming scenarios, concluding that climate-related health burdens are likely to intensify even in high-income countries.

1.1.4 Gap in the Literature

While prior research has examined the contemporaneous effects of temperature on economic output, and others have quantified the cost of poor health on lifetime economic outcomes, little is known about how temperature-induced health variation translates into long-run income losses at the individual level. Moreover, existing work often abstracts from or aggregates over individual responses.

This Master Thesis addresses this gap by quantifying the lifetime economic cost of temperature-driven health deterioration in the context of the USA, under current levels of adaptation and within a structural life-cycle framework of individual decision-making.

1.2 Research question and strategy

The economic consequences of temperature-induced health variation reflect a fundamental tradeoff embedded in individual decision-making. Higher temperatures can deteriorate health outcomes, impairing both physical capacity and cognitive functioning, which in turn depresses labor productivity and expected longevity. These changes can have long-lasting effects on income profiles, particularly when health deteriorates early in life.

Yet even in the absence of institutional responses or targeted health investments, individuals may adjust their economic behavior in response to deteri-

orating health. A worsening health trajectory may lead agents to reoptimize by altering labor supply, savings, or consumption paths. These behavioral responses—though constrained—can partially absorb the economic shock. The key question is then whether such individual adjustments are sufficient to mitigate the lifetime income loss induced by temperature-related health shocks, or whether the long-run economic cost remains substantial despite endogenous reoptimization.

This tension motivates the central research question of this paper: How do temperature-induced health shocks affect individuals' lifetime income, when only individual-level behavioral responses are allowed, and what are the economic mechanisms through which these effects propagate?

To address this question, the analysis proceeds in two stages. First, an empirical investigation quantifies the causal impact of temperature variation on individual health status. Using micro-level data, the analysis estimates how both short-term and sustained exposure to high temperatures affect health outcomes across demographic groups and age cohorts.

Second, these empirical estimates are embedded into a structural, life-cycle model of individual behavior. In the model, health enters as a state variable that evolves over time and affects both survival and future health probability distribution. Individuals maximize lifetime utility by choosing labor supply and consumption paths, taking health dynamics as exogenous but responsive to temperature. Crucially, the model does not incorporate health investment or collective adaptation, isolating the role of individual optimization.

By simulating the model under alternative temperature scenarios, the analysis computes the long-run income losses attributable to temperature-induced health shocks. These results yield a quantitative assessment of the intertemporal economic cost of climate-related health deterioration, under a benchmark of minimal adaptation.

2 Setting

This section introduces the dynamic environment in which individuals evolve over time. We provide a formal description of the mechanisms governing health and survival outcomes in response to exogenous weather realizations. The framework abstracts from individual choices and focuses on the stochastic processes linking temperature exposure, health dynamics, and mortality risk.

In each period, individuals are exposed to a realization of weather conditions. Conditional on this realization and their past health trajectory, they draw a new health status and face a probability of survival into the next period. These outcomes evolve according to reduced-form transition functions, which will later be estimated empirically.

The section proceeds as follows. The first subsection introduces the formal structure of the health and survival processes. The second subsection presents the individual-level panel data used to estimate these relationships in the subsequent section.

2.1 Formal Description

2.1.1 History Vectors

We begin by describing the framework in general terms, abstracting from empirical constraints. In this general formulation, an individual's health at time t is modeled as part of a history vector $\mathcal{H}_t \in \Omega(H)^t$, which records the sequence of health states experienced from the first period up to time t:

$$\mathcal{H}_t = (H_1, H_2, \ldots, H_t).$$

Similarly, the sequence of weather conditions encountered by an individual is captured by a weather history vector $\mathcal{W}_t \in \Omega(W)^t$:

$$\mathcal{W}_t = (W_1, W_2, \ldots, W_t).$$

These vectors serve to characterize the information available for determining health and survival outcomes at time t.

2.1.2 Health Status

Let $H_t \in \Omega(H)$ denote the health status of an individual at time t, where $\Omega(H)$ is a finite, ordered set representing possible health states. The evolution of health over time is governed by a stochastic process, with the distribution of H_t depending on the individual's prior health trajectory and experienced weather conditions.

Formally, we model health status at time t as a random draw from a conditional distribution:

$$H_t \sim f_h(\mathcal{H}_{t-1}, \mathcal{W}_t),$$

where f_h is a transition function mapping past health and current weather exposure into a probability distribution over $\Omega(H)$.

2.1.3 Living Status

Let $L_t \in \{0, 1\}$ denote the living status of an individual at time t, where $L_t = 1$ indicates survival and $L_t = 0$ indicates death in that period. Survival is modeled as a Bernoulli random variable with success probability p_t:

$$L_t \sim \mathcal{B}(p_t).$$

In the general framework, we allow the survival probability p_t to depend on an individual's full health history $\mathcal{H}_t$ and weather exposure $\mathcal{W}_t$. Accordingly, we write:

$$L_t \sim \mathcal{B}(p_t(\mathcal{H}_t, \mathcal{W}_t)).$$

This specification captures the idea that survival probabilities may be shaped by accumulated health conditions as well as contemporaneous or historical weather shocks.

In the general setting, we allow the full health and weather histories to influence subsequent transitions. However, in the empirical implementation presented later, we impose simplifying assumptions, such as using only recent health status and contemporaneous weather conditions, to improve tractability and address data limitations.

2.2 Data

This study combines three primary data sources to estimate the relationship between temperature, health, and survival outcomes. Individual-level health and mortality information is drawn from the Health and Retirement Study (HRS). Annual temperature data are obtained from the Berkeley Earth Surface Temperature project. Macroeconomic variables are sourced from the Federal Reserve Bank of St. Louis (FRED) database.

2.2.1 HRS Data

This study uses data from the Health and Retirement Study (HRS), a biennial panel survey of individuals aged 50 and older in the United States. In addition to the core survey, the HRS includes an exit interview administered to proxies of respondents who have died since the last wave. The exit survey is used to identify deceased individuals, whose living status is recorded as 0 in the year of death.

Individuals are included in the analytical sample if they were observed in the wave immediately preceding their death. To avoid confounding effects related to COVID-19 mortality, the sample is restricted to survey waves up to and including 2018. Surveys from 2000 and earlier are excluded due to inconsistent variable coding.

The final dataset includes the following variables: survey year, individual age, living status, and health status. Age is computed as the difference between the survey year and the respondent's reported year of birth. Living status is coded as 1 if the individual appears in the main survey and 0 if they appear only in the exit survey. Health status for deceased individuals is imputed from their most recent observation prior to death.

Health is proxied using a self-reported categorical measure consistently available across all survey waves. Respondents are asked to classify their general health into one of five categories: *Excellent*, *Very Good*, *Good*, *Fair*, or *Poor*. Responses coded as 8, –8, or 9, corresponding to missing, non-response, or refusal, were excluded from the final sample. They represented less than 30 observations in total and are not expected to materially affect the analysis. Although self-reported health lacks the precision of composite indices based on clinical markers, prior studies have shown it to be highly correlated with both morbidity and mortality. Its availability across all waves and simplicity of interpretation make it a tractable measure of overall health status in this context.

In addition, the secondary health proxy, $HP_{i,t}$, is constructed using binary indicators for four self-reported chronic conditions: *high blood pressure*, *lung disease*, *heart condition*, and *stroke*.

Figure 1 provides an overview of the health status distribution over time. Each bar corresponds to a survey wave, with segment colors indicating the number of individuals reporting each health status category. Unlike proportion-based plots, which normalize distributions, this count-based representation highlights both the evolution of health composition and the variation in the number of observations across survey waves.

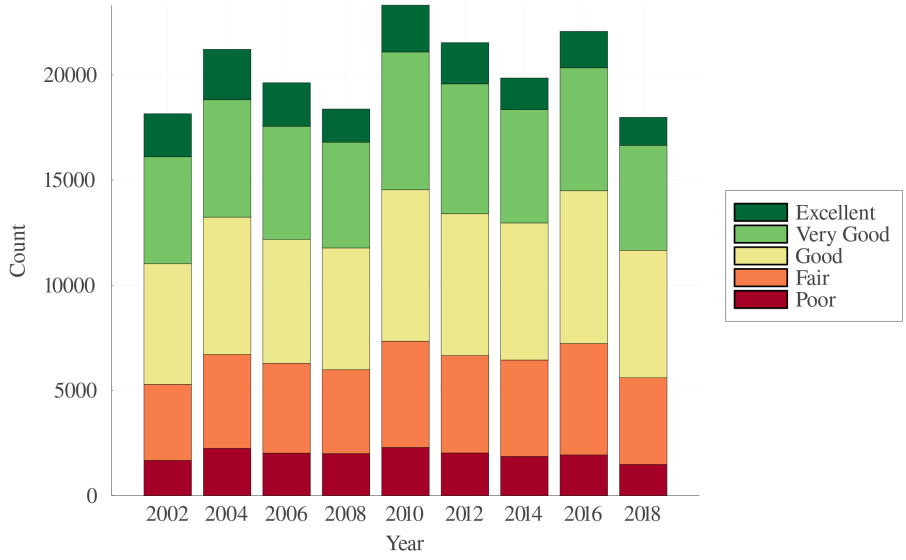

Figure 1: Health Status distribution per Year, from the HRS data.

2.2.2 Climate Data

Temperature data are drawn from the Berkeley Earth project's *Land Monthly Average Temperature* dataset, which reports monthly global land surface temperature anomalies through time. Anomalies are measured relative to the 1951–1980 baseline, with 95% confidence bounds provided for each month. Figure 2 shows the upward trend in global average land temperature over time.

The analysis uses global average annual temperature as the climatic variable. This measure offers a tractable and transparent proxy, avoiding the complexity of regional variation while remaining informative.

Four temperature trajectories are considered for simulation. The *historical path* rises from 0 to 1.5°C between the mid-20th and mid-21st century. Three additional scenarios, drawn from IPCC projections for 2000–2100 and starting

at 0.5°C, reflect broader possibilities: a *pessimistic path* reaching 4°C, an *intermediate path* reaching 3°C, and an *optimistic path* stabilizing at 2°C. These benchmark paths allow for structured comparisons of long-run effects on health and income.

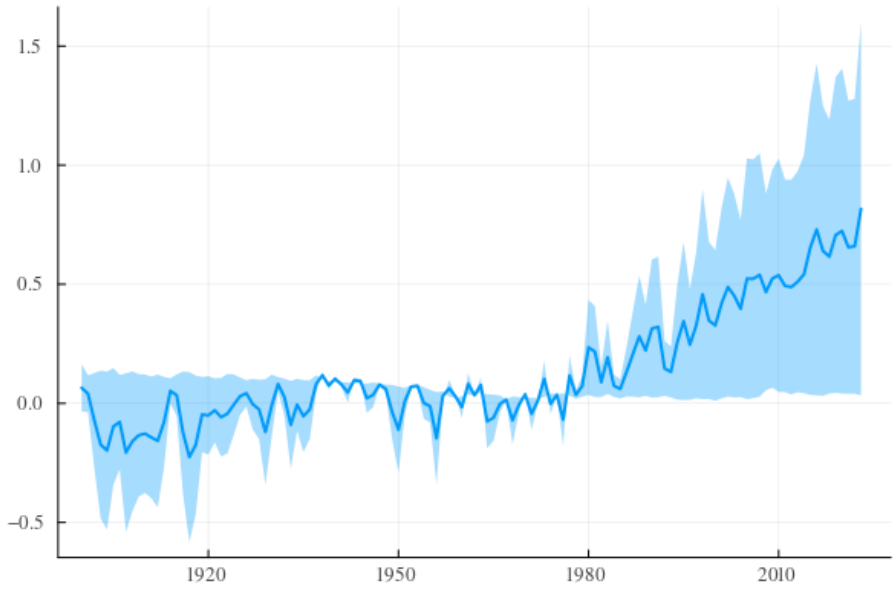

Figure 2: Evolution of Global Average Annual Temperature (1900–2022)

The dark blue line plots the global average temperature anomaly relative to the 1951–1980 baseline. The light blue shaded area shows the 95% confidence interval around each year's estimate, as provided by the Berkeley Earth dataset.

2.2.3 Economic Data

Finally, economic data from the Federal Reserve Bank of St. Louis (FRED) are used for two purposes. Annual U.S. Gross Domestic Product (GDP) figures are employed in preliminary estimation exercises, while the long-run average interest rate is used to calibrate the discount factor in the economic model.

3 Estimation of Health and Survival Dynamics

This section presents the empirical framework used to estimate the relationships between temperature, individual health trajectories, and survival probabilities. Using microdata from the Health and Retirement Study (HRS), we focus on modeling health transitions and mortality risk as functions of recent health status, temperature exposure, and age.

We begin by modeling health dynamics through an ordered response approach that leverages the five-category self-reported health variable. We then estimate survival probabilities using a binary outcome model, again accounting for health and temperature effects. To address concerns of omitted variable bias and potential collinearity, we introduce a Health Proxy, which allows for a tractable way to represent how temperature might affect transitions via acute health risks.

The resulting estimates capture a reduced-form effect of climate variation on health and survival, through a group of health risk, and serve as key inputs for the economic model introduced in the next section.

3.1 Health Transition

The Health and Retirement Study (HRS) provides detailed longitudinal data on individuals' self-reported health, captured across five ordered categories. To preserve the richness of this variable, it is not recoded into a binary indicator (e.g., "Good" vs. "Bad") but retained in its full ordinal form, with $H \in \{1, \ldots, 5\}$ representing states from "Excellent" to "Poor" health.

Given the ordered and discrete nature of the outcome, health transitions are modeled using ordered response models—specifically, the ordered logit and ordered probit—due to their tractability and widespread use in the literature.

For computational and identification reasons, we restrict the information set determining current health status to the most recent lag and contemporaneous temperature. That is, rather than modeling the full dependence $f_h(\mathcal{H}_{t-1}, \mathcal{W}_t)$, we simplify the transition function to:

$$f_h(H_{t-1}, T_t),$$

where T_t is the average annual temperature at time t.

Since health status takes values in a finite, ordered set, f_h defines a categorical distribution (sometimes referred to as a generalized Bernoulli), and can be expressed as a transition function indexed by previous health status:

$$f_h(H_{t-1} = j, T_t) = f_{h,j}(T_t), \quad \forall j \in \{1, \ldots, 5\}.$$

To estimate these transition probabilities, one could consider a direct ordered logistic regression with H_t as the dependent variable, and age, temperature, and other controls as covariates. However, this naive approach faces two major challenges. First, omitted variable bias: many unobserved factors, such as access to care or behavioral choices, can affect both health and survival. Second, collinearity: economic controls (such as GDP or health expenditures) are often strongly correlated with temperature trends, making it difficult to isolate causal effects.

Moreover, interaction effects between covariates are likely important. For example, the impact of a given health state on future transitions may differ substantially by age: "Fair" health at age 30 has different implications than at age 80.

To address these concerns, we introduce an two-staged-regression inspired strategy.

We define a composite health shock measure, the *Health Proxy* ($HP_{i,t}$), capturing the burden of recent temperature-sensitive health incidents. This proxy is constructed as the sum of binary indicators for the presence of the following four health conditions: *High blood pressure*, *Lung disease*, *Heart condition*, *Stroke*. Formally:

$$HP_{i,t} = \text{HighBP}_{i,t} + \text{Lung}_{i,t} + \text{Heart}_{i,t} + \text{Stroke}_{i,t}$$

We first estimate a linear model for $HP_{i,t}$ as a function of age and temperature:

$$\widehat{HP}^{I}_{i,t} = \widehat{\beta_0} + \widehat{\beta_A} \cdot \text{Age}_{i,t} + \widehat{\beta_T} \cdot T_t + \widehat{\beta_{A\times T}} \cdot (\text{Age}_{i,t} \times T_t)$$

This first-stage regression provides a filtered proxy for temperature-induced health risks, which is then used in a second regression to estimate health transition probabilities. Specifically, we regress the probability of transitioning to a new health state on previous health status and the predicted health proxy $\widehat{HP}^{I}_{i,t}$, thus controlling for age and filtering out temperature's indirect effects via acute health events. This two-step strategy allows us to better identify the effect of temperature on acute health state dynamics while mitigating omitted variable bias and accounting for age interactions.

The first-stage regression results, presented in Table 1, provide empirical support for the construction of the Health Proxy as a function of age, temperature, and their interaction. As expected, age is a strong and significant predictor of acute health conditions, with each additional year associated with a 0.02 increase in the composite health burden measure ($p < 0.001$). The standalone effect of temperature is negative but statistically insignificant, suggesting that average annual temperature alone does not systematically explain acute health conditions in this sample. However, the interaction term between age and temperature is positive and statistically significant at the 1% level. This indicates that the effect of temperature on health burden intensifies with age—a key channel motivating the use of $\widehat{HP}^{I}_{i,t}$ as a mediator in the second stage. While the model explains only a modest portion of the variance in health conditions ($R^2 = 0.086$), this is expected given the many unobserved factors—such as genetic predisposition, lifestyle, or access to care—that drive acute health events. However, our primary goal is not to fully explain health shocks, but rather to isolate the marginal effects of temperature and age. In that respect, the significant interaction between age and temperature supports the interpretation of the Health Proxy as a temperature-sensitive health shock, particularly among older individuals.

	HP
(Intercept)	-0.487***
	(0.068)
Age	0.020***
	(0.001)
Temperature	-0.032
	(0.123)
Age × Temperature	0.005**
	(0.002)
N	182,947
R^2	0.086

Table 1: Regression of Health Proxy on Age, Temperature, and their interaction.

Estimated Health Transition Probabilities. The two following figures depict the estimated probabilities of transitioning across self-reported health states as a function of age, conditional on the current health status. The five health categories considered are *Excellent*, *Very Good*, *Good*, *Fair*, and *Poor*. These transition probabilities provide a dynamic picture of health deterioration (or improvement) over the life cycle. For clarity purposes, temperature was not included in these graphics to avoid 3D plotting. [1]

From excellent health, the probability of remaining in this health state declines steadily with age, while the proba bility of transitioning to Very Good health increases. Transitions to lower health states (Good, Fair, Poor) remain unlikely but grow slowly over time. This indicates that while aging naturally erodes top health status, the decline is gradual and dominated by moves to slightly lower but still positive states.

[1] Further graphical representations of transition probabilities are available in the Appendix.

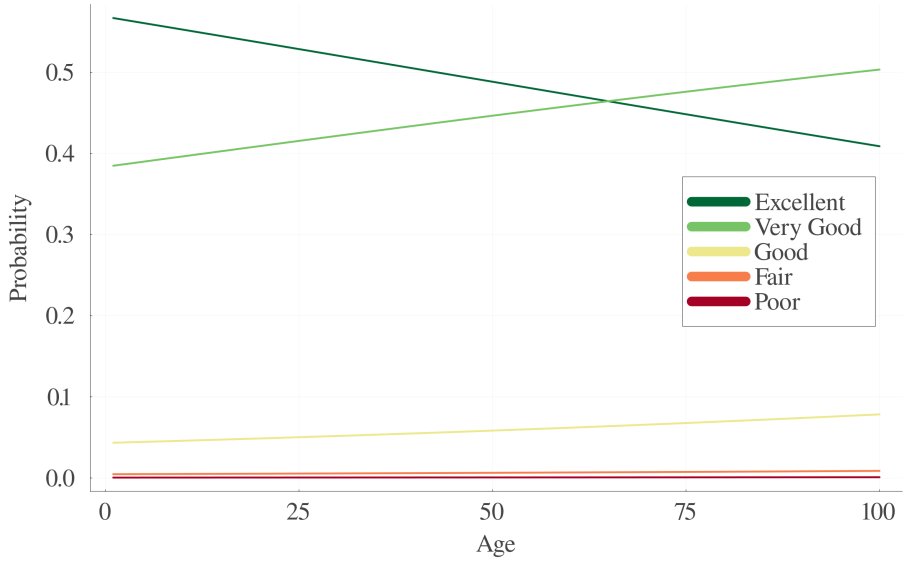

Figure 3: Transition probabilities from Excellent Health

In the opposite case, the probability of remaining in *Poor* health increases markedly with age, surpassing 60% by age 100. Improvements to better health categories become virtually negligible with age, suggesting that *Poor* health is largely an absorbing state for older individuals.

These estimated transition probabilities highlight the persistent and age-dependent nature of health status. They support the modeling assumption of a health process that becomes increasingly inertial with age, and they reflect the empirical reality that upward health mobility becomes rarer in older populations. This framework is essential for evaluating how external shocks—such as temperature-driven health shocks—interact with baseline health dynamics across the life cycle. Based on these estimates, it is alread possible to perform simulations of different groups of individuals with specific temperature trajectories. [2]

3.2 Living Status

The binary nature of the living status variable allows for a straightforward application of logistic regression.

To estimate the survival probability $p_t(\mathcal{H}_t, \mathcal{W}_t)$, a naive regression approach would encounter similar issues to those previously discussed. For instance, estimating a regression using only GDP as a covariate leads to a negative coefficient

[2] A specific illustration is available in the Appendix.

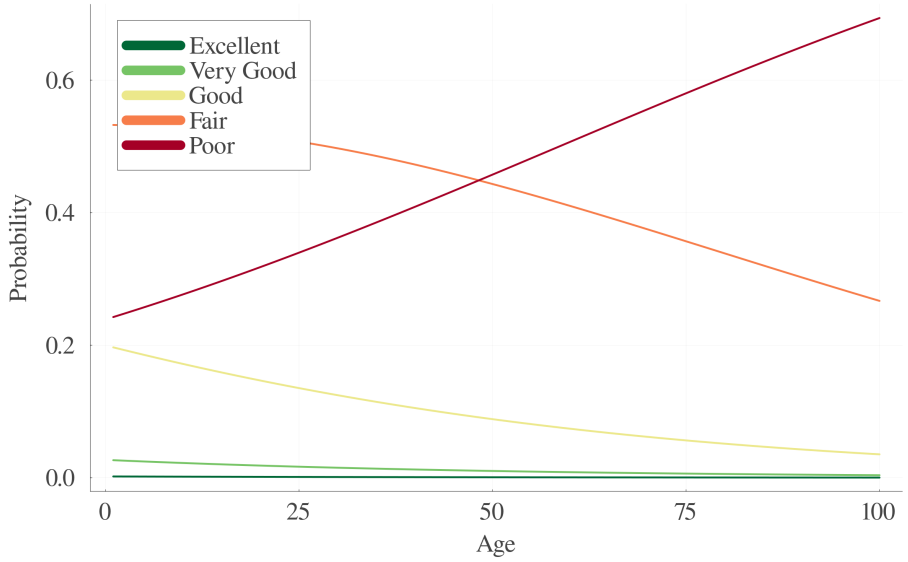

Figure 4: Transition probabilities from Poor Health

not only on temperature but also on GDP. This counterintuitive result reflects a recent trend in the United States, where GDP has continued to grow substantially, while life expectancy has remained stagnant or slightly declined. As such, preliminary results showed the necessity of adapting the regression specification, as it is done by the Health Proxy $HP_{i,t}$, as explained above.

Using the logistic function $\Lambda(\cdot)$, we estimate the individual survival probability $p_{i,t}$ at time t via the following specification, which incorporates the previously estimated health proxy $\widehat{HP}^{I}_{i,t}$:

$$\widehat{p_{i,t}} = \Lambda\left(\widehat{\beta_0} + \widehat{\beta_H} \cdot Health_{i,t} + \widehat{\beta_{HP}} \cdot \widehat{HP}^{I}_{i,t}\right) \tag{1}$$

By combining the health transition probabilities with these survival probability estimates, we can simulate and visualize the demographic dynamics of a population over time. This is illustrated in the next figure, which shows the annual survival probability as a function of both age and health status, based on an initial population of $N_0 = 10{,}000$.

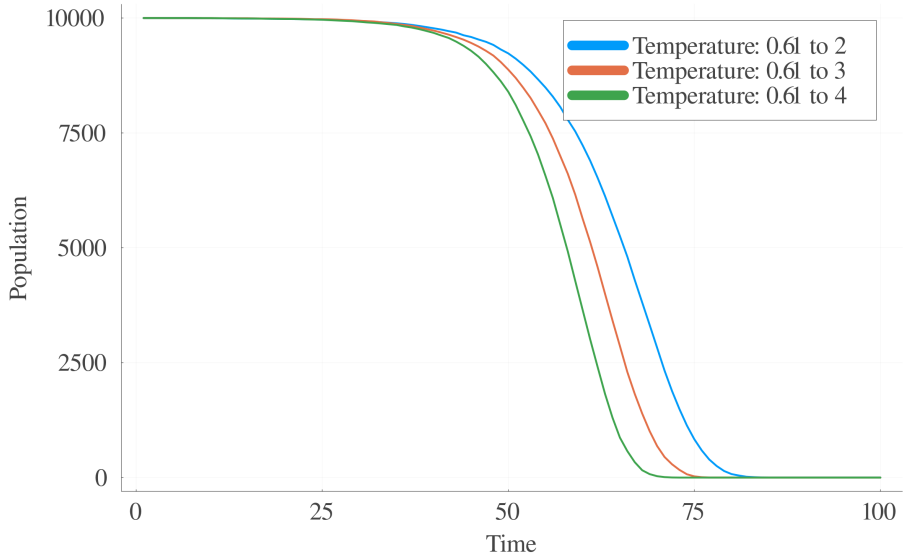

Figure 5: Annual probability of survival as a function of age and health status, obtained with $N_0 = 10{,}000$.

Higher temperatures can exacerbate acute health conditions, particularly among vulnerable populations such as the elderly or those with pre-existing health issues. For instance, extreme heat has been linked to cardiovascular stress, respiratory complications, and increased incidence of heat-related illnesses. These acute conditions can accelerate transitions from better to worse health states and elevate mortality risk. Furthermore, temperature interacts with age in a non-linear fashion. Older individuals generally have reduced thermoregulatory capacity, making them more susceptible to heat stress. As a result, even moderate increases in temperature can disproportionately affect their survival probabilities and hasten deterioration in health status. Therefore, the negative coefficient on temperature is not merely a statistical artifact but reflects real physiological and epidemiological mechanisms. This compound influence (affecting both the likelihood of transitioning to a worse health state and the immediate probability of survival) drives the overall negative relationship between temperature and life expectancy observed in our model.

These estimates are now going to be used in the economic model.

4 Model

This section is dedicated to the formal description of the model, as well as its analytical analysis. First, its main mechanisms will be explained, and then, the inexistence of analytical solution in most cases will be shown.

4.1 Baseline specification

The agents maximizes:

$$\max_{\{c_t, l_t, s_{t+1}\}_{t=1}^{100}} \mathbb{E}\left[\sum_{t=1}^{100} \beta^t \cdot u(c_t, l_t)\right]$$

Their utility function is:

$$u(c_t, l_t) = \frac{c_t^{1-\rho}}{1-\rho} - \xi_t \cdot \frac{l_t^{1+\varphi}}{1+\varphi}$$

With :
- c_t the consumption
- l_t the quantity of labor supply provided by the agent
- h_t the health status
- w_t the weather variable, which is here temperature
- ξ_t the labor disutility coefficient
- ρ the risk aversion coefficient
- φ the Frisch elasticity of Labor supply.

The agent is subject to the following budget constraint:

$$c_t + s_{t+1} \leq l_t \cdot z_t + s_t \cdot (1 + r_t)$$

With:
- c_t the consumption at period t
- s_{t+1} the savings for period $t+1$
- l_t the labor supply provided by the agent at period t
- z_t the productivity at time t
- s_t the savings available at the beginning of period t
- r_t the interest rate at period t

Also, agents are subject to the following borrowing constraint, defined as:

$$s_{t+1} \geq \underline{s}, \forall t \in [\![1, T]\!]$$

We can note the First Order Conditions, such that:

$$c_t^{-\rho} \cdot z_t = \xi_t \cdot l_t^{\varphi} \iff \begin{cases} c_t = \left[\frac{\xi_t \cdot l_t^{\varphi}}{z_t}\right]^{-\frac{1}{\rho}} \\ l_t = \left[\frac{c_t^{-\rho} z_t \cdot}{\xi_t}\right]^{\frac{1}{\rho}} \end{cases} \tag{2}$$

And

$$c_t^{-\rho} = \beta \cdot \mathbb{E}\left[c_{t+1}^{-\rho} \cdot (1 + r_{t+1})\right] + \gamma_t \tag{3}$$

The first corresponds to the equalization of marginal benefit and cost of labor, and the second corresponds to the Euler equation.

The first equilbrium condition implies an within decision, driven by the labor disutility coefficient ξ and the productivity z. There is a unique mapping

between consumption and labor at any period, to equalize the benefits and the costs of labor.

The second equilibrium condition implies an intertemporal decision. The marginal utility of consumption at one period must be equal to the expected marginal utility of conusmption next period, discounted by the discounting factor β and the interest rate next period $(1 + r_{t+1})$, plus the marginal benefit of violating the borrowing constraint at the current period.

It is now important to describe what the Expectation operator $\mathbb{E}$ entails here. In a generic formulation, one could expect the uncertainty to affect the interest rate at the next period, which is the reason $(1 + r_{t+1})$ is within the operator.

Another specification could exclude any uncertainty from the interest rate. The uncertainty could then come from the health and survival draw. If the uncertainty only comes from these two draws, the expectation operator can be formalized such as:

$$\mathbb{E}\left[c_{t+1}\right] \equiv p_{t+1}(\mathcal{H}_t, \mathcal{W}_t) \cdot c_{t+1}$$

4.2 Analytical Solution Inexistence

Proposition This maximization program is impossible to solve analytically in most cases[3].

If we consider the model altogether, it is impossible to describe analytically the optimal policy functions of the three choice variables. While the entire proof is available in the appendix, a quick explanation is possible here. First, the objective functions is linear with the savings at next period s_{t+1}, making it disappear from the F.O.C.s. This term requires therefore the labor and consumption policies to be solved, and then plugged into the budget constraint, to have a solution. However, if we try to solve the two other policy functions, we end up with transcendantal equations of the form $a \cdot x^{\alpha} + b \cdot x + c = 0$, with $\alpha \notin \mathbb{N}$. This transcendantal equations can be overcome with specific combinations of parameters, but these are however absurd in our context. This inexistence of analytical solution calls henceforth for a numerical solving of the model. The next section discusses the different methods used in order to do so.

5 Numerical methods

Several ways have been considered to solve this model numerically. This section is dedicated to the presentation of the different methods used in order to do so. First, the auxiliary functions are presented. Second, the different main algorithms specifications and their performance are presented. Finally, the aggregation methods and different numerical results are discussed.

[3]The proof of this proposition is in the Appendix.

5.1 Functions

This subsection is dedicated to the description of the fundamental programmatic functions that were used to solve the model numerically.

- **Budget clearing function:** The budget clearing function computes the amount of non used income for a set of state and choice variables. Since at optimal, the budget constraint is binding, the underlying theoreical result indicates that the budget clearing function should be zero. Given the imprecision of numerical methods, the average budget clearing function was used as a measure of the precision performance of each algorithm.

  It is equal to:

$$B(s_t, l_t, c_t, s_{t+1}) = l_t \cdot z_t + s_t \cdot (1 + r_t) - s_{t+1} - c_t$$

- **Bellman function:** The Bellman function takes as an argument the value function next period, and maximizes the current utility plus the discounted value function next period.

  It is equal to:

$$V(s_t) = \max_{\{c_t, l_t, s_{t+1}\} \in \Gamma(s_t)} \{u(c_t, l_t) + \beta \cdot V(s_{t+1})\}$$

  With $\Gamma(s_t)$ the feasibility set given by the state variable s_t.

- **Backwards function:** The backwards function iterates the Bellman function from the last period to the first one. In the case of policy iteration, it iterates over the policy function, and not the value function. It aggregates the optimal decisions and returns a grid of optimal choices associated to each period and state variable value.

  For the pure numerical value function iteration, the backwards function is as following:

```
for t from 100 to 1

    if t is equal to 100
        Bellman next period = Vector of zeros
    end

    for s in the possible set of s
        for c,l,s' in the feasible set of the current s value

            # We compute the budget clearing:

            bc = budget_clearing(c,l,s')

            # If it does not,
            # we set the value function to a very low number.

            if bc < 0

                V[c,l,s',s] = -Inf

            # If it does, we compute the value function
            # for this combination of choice variables.

            else if bc >= 0

                V[c,l,s',s] =
                    utility(c,l,s') +
                    beta * probability of survival *
                    Bellman next period[s']
            end
        end

        # We set the value function for s and t to
        # the maximum value found.

    end

# We set the value function at next period to current one
Bellman_next_period = Value_function[index_s,t]

end
```

Figure 6: Pseudo-code of the backward function.

5.2 Algorithms

This section details the different algorithms built upon the above-mentioned fundamental functions. Indeed, if one can think of the pure numerical value function

iteration to solve the model, multiple approaches exist, that vary depending on the targeted tradeoff between precision performance and speed performance[4].

5.2.1 Pure numerical value function iteration

The pure numerical value function iteration algorithm consists in verifying all possible combination of choice variables for each level of state variable to determine what is the best possible response given a certain amount of state variable.

Here, the algorithm goes through all the possible values of c, l, and s', without using any approximation obtained through the FOC mentioned above. This is quite computational-intensive, but has the advantage of not using analytical results, which can lead to approximation depending on the resolution of the ranges used.

5.2.2 F.O.C. approximated value function iteration

The FOC approximated value function iteration algorithms make use of the two expression of consumption and labor supply derived from the FOC seen in the previous section. They are faster by order of magnitudes when compared to the pure numerical value function iteration algorithm, but contain more errors, measured by the budget clearing function[5].

5.2.3 Interpolated algorithms

The interpolated algorithms use interpolation techniques to approximate the value of the next period Bellman equation. This interpolation can be implemented in the pure numerical algorithm, and in the FOC-approximated ones.

They allow for a smoother shape of policy function, and have graphical results that are more easily interpretable. However, their speed performance is slightly worse, and the effect of interpolation on precision performance is ambiguous.

[4]For more information, the different steps of the algorithms and their source code are available online. The steps and comments of the present work are available here: `https://www.paulogcd.com/Master_Thesis/`, and the documented replication package, coded in Julia, is available here: `https://www.paulogcd.com/Master_Thesis_Paulogcd_2025/`.

[5]Note that it is impossible to use the second FOC, i.e. the Euler equation, containing the Lagrangien multiplier γ_t. However, the numerical solving process allows for an estimation of γ_t.

5.3 Performance

Algorithm	Error	Time (in seconds)	Memory (in Mb)
Pure Numerical Value Function Iteration	0.0179	0.6604	1033.4409
FOC approximation 1 (fixing labor supply)	0.042	0.2506	98.1834
FOC approximation 2 (fixing consumption)	0.042	0.0188	55.6981

Figure 7: Algorithms and their performance.
These results were obtained from reduced ranges, but scale exponentially.

5.4 Policy Function Results

This subsection is dedicated to the presentation of the policy function results from the numerical methods.

The calibration was done following the used in the found literature, and in order to make the numerical resolution possible. The interest rate and discount factor were obtained after averaging the past interest rate, from the FRED data mentioned previously.

Table 2: Model Parameter Values

Parameter	**Value**
Risk aversion coefficient (ρ)	1.50
Labor supply Frisch elasticity (φ)	2.00
Discount factor (β)	$\frac{1}{1+r} \approx 0.9825$
Annual interest rate (r)	0.0178 (1.78%)

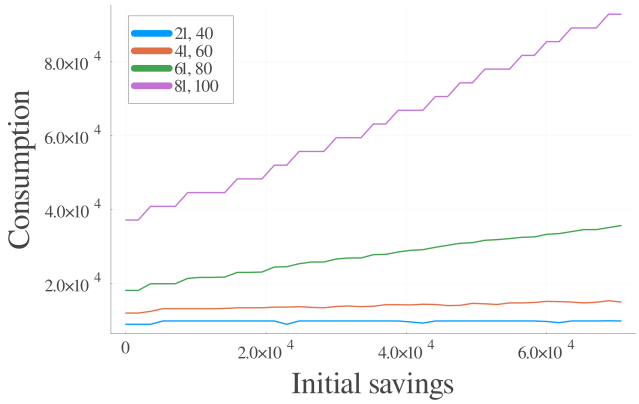

Figure 8: Consumption policy per age category obtained from the pure numerical value function iteration

The labor policy shows the increasing effect of age on the elasticity between savings and labor income, due to decreasing survival probabilities.

The savings policy is decreasing with age, reflecting the lower survival probabitilies as the agents become older. In the last years, the agents desave, and tend to consume everything they have left.

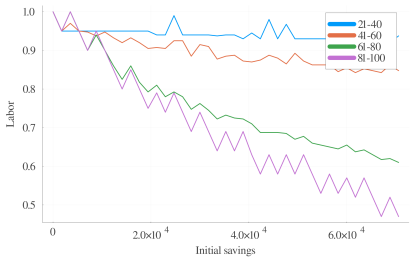

Figure 9: Labor policy per age category

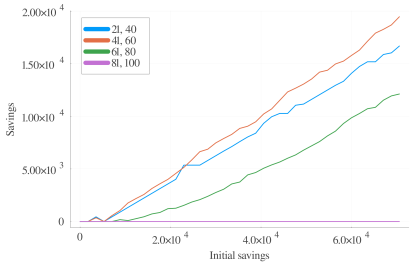

Figure 10: Savings policy per age category

6 Results

This section is dedicated to the presentation of the results of the comparison of the life time income between agents in different temperature scenarios.

6.1 Lifetime income

To perform a comparison between different temperatures scenarios, we first need to precisely characterized the comparison reference, i.e. the lifetime income.

A simulation was conducted using a projected temperature trajectory ranging from 0.00 to 1.50 degrees Celsius. This range approximately reflects the temperature increase experienced by the cohort born in the 1950s.

According to data from PMCID: PMC4534330, the estimated lifetime earnings (in 2020 dollars) for individuals with less than a high school education (LTHS) are $1,178,000 for men and $586,000 for women, yielding an average of approximately $882,000. For high school graduates, the corresponding figures are $1,825,000 for men and $1,351,000 for women.

In light of these benchmarks, a reference value of $1.45 million was selected to represent a moderate level of lifetime earnings. This serves as the baseline for estimating the economic consequences of temperature-related health shocks over the lifespan of this cohort.

It is important to note, however, that this estimate likely understates the true cost of such shocks. The Health and Retirement Study (HRS) data used in the health transition modeling includes a broader and more educated sample than the average LTHS population. Numerous studies have established that higher educational attainment is associated with improved health outcomes and longer life expectancy. As a result, the health impacts derived from the HRS data are expected to be less severe than those experienced by less educated individuals. Consequently, the simulated economic burden associated with temperature-induced health deterioration may be conservatively estimated.

6.2 Comparison

This subsection is dedicated to the comparison between populations having different temperature trajectories.

First, survival probabilities will be compared, then, the policy functions will be compared (consumption, labor, savings). Finally, the lifetime income will be compared.

The 4 temperature trajectories compared are:

- The past temperature trajectory: From 0.01 to 1.5
- The optimistic scenario: From 0.61 to 2.0
- The intermediate scenario: From 0.61 to 3.0
- The pessimistic scenario: From 0.61 to 4.0

6.2.1 Demographic comparison

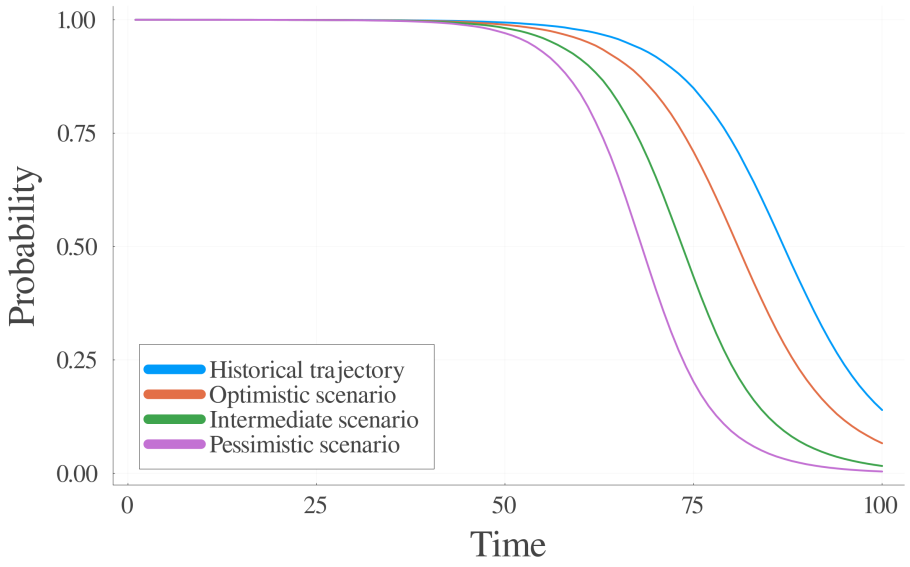

Figure 11: Savings policy per age category obtained from the pure numerical value function iteration

6.2.2 Policy functions comparison

One possible way to compare policy functions across populations are the computation of a policy function average throughout all ages.

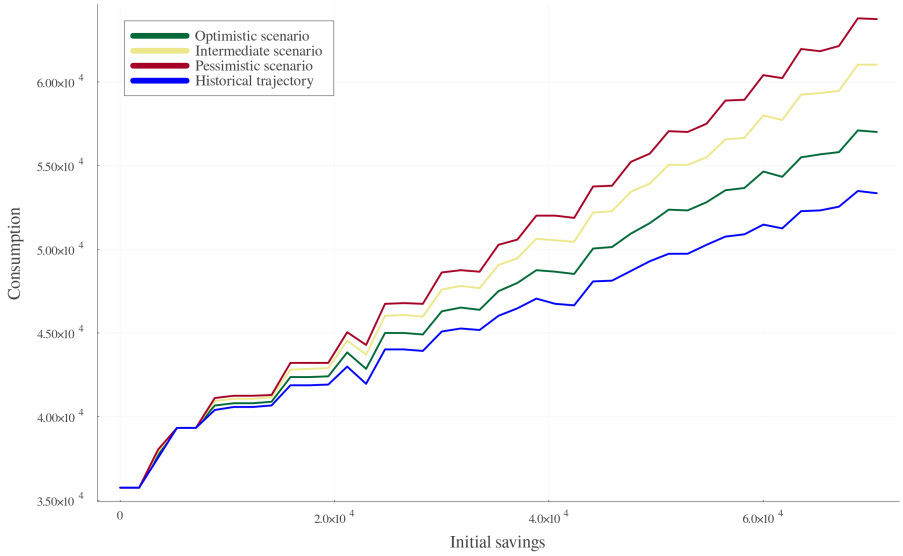

Figure 12: Consumption policy comparison

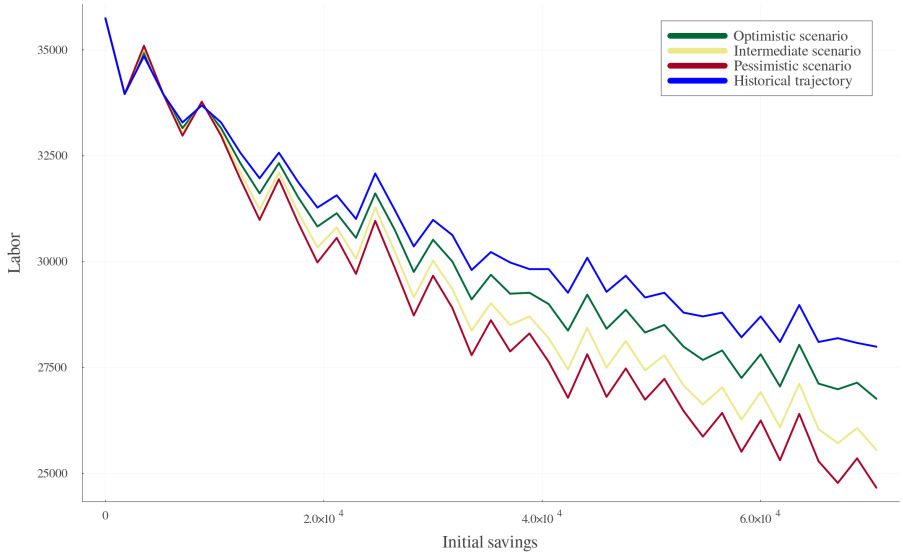

Figure 13: Labor policy comparison

The comparison of optimal policy paths across varying temperature trajecto-

ries reveals a discernible deadweight loss attributable to demographic dynamics. Specifically, this loss arises from temperature-induced shifts in survival probabilities over time. As higher temperatures adversely affect health transitions and increase mortality risk (particularly among older or more vulnerable individuals) the resulting demographic structure alters the expected lifetime utility and economic behavior of agents.

This demographic distortion reduces the effectiveness of policy instruments optimized under baseline conditions, thereby generating inefficiencies. The magnitude of the deadweight loss reflects both the direct impact of elevated temperatures on survival probabilities and the indirect effect on population composition, labor force participation, and the intertemporal allocation of resources. In this context, the demographic channel becomes a critical mechanism through which climate change translates into long-term economic costs, even in the absence of immediate productivity shocks.

6.2.3 Lifetime income comparison

The deterioration in lifetime income resulting from temperature-related health shocks is substantial and operates through multiple, compounding channels. Elevated temperatures are empirically associated with a higher incidence of acute health events—such as cardiovascular and respiratory crises—that not only increase short-term morbidity and mortality but also reduce long-term functional capacity. These effects are particularly pronounced among older adults and individuals in fragile health, whose ability to remain in the labor force or engage in productive activities declines disproportionately.

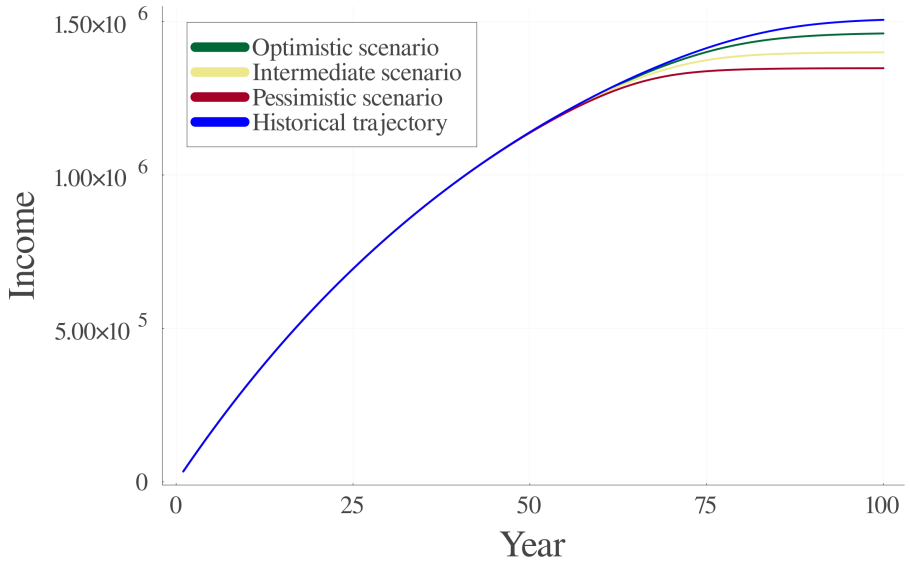

Figure 14: Expected lifetime labor income, at each period.

Simulations suggest that even modest increases in average temperature over the life course can translate into significant reductions in expected lifetime income. This arises not only from premature mortality but also from suboptimal health states that lower utility and earning potential throughout the individual's remaining life. Therefore, the macroeconomic cost of climate-related health deterioration should be understood as not merely a public health challenge but a fundamental constraint on human capital and economic resilience. In this sense, the lifetime income loss induced by change in survival probabilities due to acute health conditions provoked by temperature changes amounts to approximately $110,000 of 2020, when taking the lifetime income of the High School Graduates of the 1950s generation ($1.45 Mio) as the reference point.

7 Discussion

This paper quantifies the lifetime economic cost of temperature-induced health deterioration by integrating empirical estimates of health and survival dynamics into a structural life-cycle model. The results highlight two key mechanisms: (1) temperature-driven health shocks reduce survival probabilities, particularly among older and vulnerable populations, and (2) these shocks propagate through individual adjustments in labor supply, savings, and consumption, culminating in significant lifetime income losses (approximately $110,000 per capita under pessimistic warming scenarios).

The estimated policy functions align with life-cycle theory: savings peak

in mid-life and decumulate with age, while labor supply declines as health deteriorates. This attempts to complement the literature on climate-economy feedbacks (Burke et al., 2015; Bilal & Kanzig, 2024) by isolating the role of health-mediated channels absent collective adaptation.

The empirical health transitions, estimated via a two-stage ordered-response framework, confirm that temperature exacerbates acute conditions (e.g., cardiovascular stress) and accelerates transitions to poorer health states. This mirrors findings by Barreca et al. (2016) on temperature-mortality adaptation but extends them to the economic individual choices.

7.1 Limitations

This present work suffers however from multiple methodological limitations.

First, by its health measure methodology. This limitation is twofolds. First, due to the reliance on the Self-Reported Health. This reliance may understate severe clinical conditions. Future work could integrate biomarkers (e.g., NHANES data) to capture latent health risks. Second, due to the limitations of the proposed and used Health Proxy, that does not capture fully neither isolate perfectly the effect of temperature on health.

Another important limitation of this work comes from its integration of temperature variability: Using annual averages masks acute shocks (e.g., heatwaves), which may have nonlinear effects on health (IPCC, 2022). High-frequency data could refine the health proxy.

The third major flaw of this work is its abstraction from general equilibrium effects (e.g., wage adjustments, health investment). A richer framework could include endogenous labor demand or public adaptation policies.

Finally, it could be interesting to introduce educational heterogeneity for two reasons. Not only would it create heterogeneity at the productivity level, but it would also interact with the health and survival probabilities. Furthermore, the baseline lifetime income estimate ($1.45M) likely understates costs for less-educated groups, who face higher climate vulnerability (Deryugina & Hsiang, 2017). Disaggregating by socioeconomic status could be a priority for future research.

By bridging health dynamics, macroeconomic economics, and dynamic optimization together, the present work propose a framework in which temperature-induced health shocks impose economically meaningful costs through both mortality and morbidity.

8 References

9 Appendix

9.1 Health Transition Probabilities

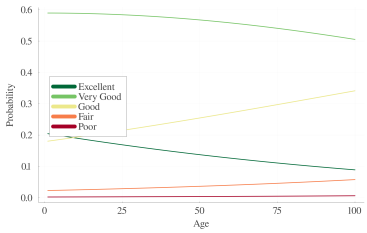

Figure 15: Transition probabilities from Very Good Health

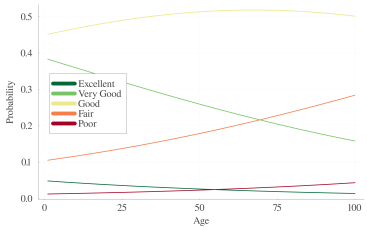

Figure 16: Transition probabilities from Good Health

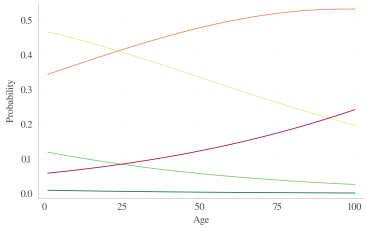

Figure 17: Transition probabilities from Fair Health

9.2 Health simulation

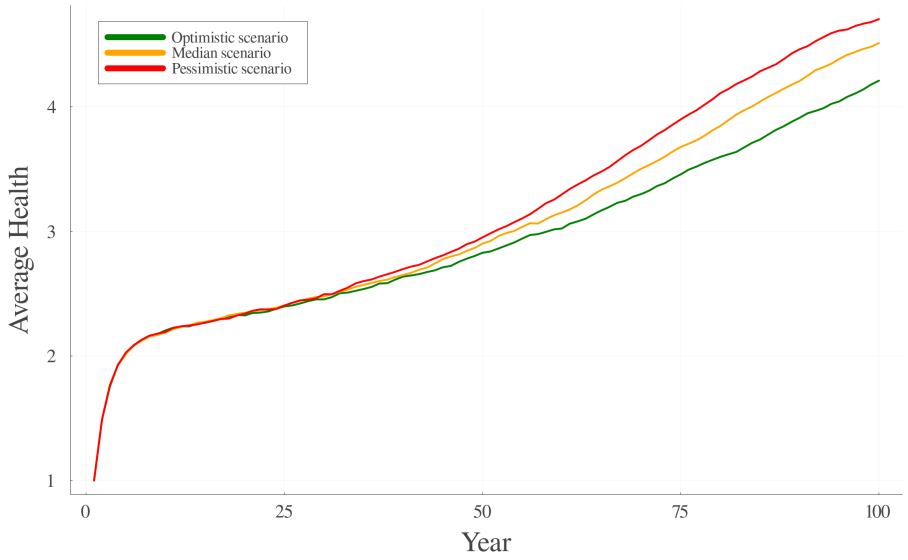

Figure 18: Annual average health status as a function of temperature scenarios.

9.3 Proof of Impossibility

This section is dedicated to the proof that the maximization program has no analytical solution in most cases.

We will show this absence of analytical solution by attempting to solve it in three different ways: First by using the Budget Constraint binding, then by using the F.O.C. and the Budget Constraint, and lastly trying to go to the last period to solve it recursively.

9.3.1 Maximization program

$$\max_{\{c_t, l_t, s_{t+1}\}_{t=1}^{100}} \mathbb{E}\left[\sum_{t=1}^{100} \beta^t \cdot \frac{c_t^{1-\rho}}{1-\rho} - \xi_t \cdot \frac{l_t^{1+\varphi}}{1+\varphi}\right]$$

Subject to budget and borrowing constraints:

$$c_t + s_{t+1} \leq l_t \cdot z_t + s_t \cdot (1 + r_t)$$

$$s_{t+1} \geq \underline{s}, \forall t \in [\![1, 100]\!]$$

9.3.2 Budget constraint binding

A first solving attempt consists in assuming that the budget constraint binds. We can then obtain the following expression for consumption:

$$c_t = l_t \cdot z_t + s_t \cdot (1 + r_t) - s_{t+1}$$

Plugging it into the maximization program, we obtain:

$$\max_{\{l_t, s_{t+1}\}_{t=1}^{100}} \mathbb{E}\left[\sum_{t=1}^{100} \beta^t \cdot \frac{(l_t \cdot z_t + s_t \cdot (1 + r_t) - s_{t+1})^{1-\rho}}{1-\rho} - \xi_t \cdot \frac{l_t^{1+\varphi}}{1+\varphi}\right]$$

The F.O.C. with respect to labor implies:

$$l_t^{\varphi} \cdot \xi_t = [l_t \cdot z_t + s_t \cdot (1 + r_t) - s_{t+1}]^{-\rho} \cdot z_t \tag{4}$$

We can develop the decomposition of consumption if and only if $\rho \in \mathbb{N}$. Indeed, this equation is of form $x = (x-\alpha)^{\beta} \cdot z$. With $\beta \notin \mathbb{N}$, is a transcendantal equation.

9.3.3 F.O.C. and Budget clearing

We can now try to compute the F.O.C. first, and then make use of the Budget Constraint. The Lagrangien function associated witht the maximization program of the agent is:

$$\begin{aligned}\mathcal{L}(c_t, l_t, s_{t+1}; \lambda_t, \gamma_t) = \mathbb{E}\Big[\sum_{t=1}^{100} \beta^t \cdot ((&\frac{c_t^{1-\rho}}{1-\rho} - \xi_t \cdot \frac{l_t^{1+\varphi}}{1+\varphi}) \\ &+ \lambda_t \cdot (l_t \cdot z_t + s_t \cdot (1 + r_t) - c_t - s_{t+1}) \\ &+ \gamma_t \cdot (s_{t+1} - \underline{s}))\Big]\end{aligned} \tag{5}$$

The First Order Conditions are the following:

$$\frac{\partial \mathcal{L}}{\partial c_t} = 0 \iff c_t^{-\rho} = \lambda_t$$

$$\frac{\partial \mathcal{L}}{\partial l_t} = 0 \iff \lambda_t \cdot z_t = \xi_t \cdot l_t^{\varphi}$$

$$\frac{\partial \mathcal{L}}{\partial s_{t+1}} = 0 \iff \lambda_t = \beta \cdot \mathbb{E}\left[\lambda_{t+1} \cdot (1 + r_{t+1})\right] + \gamma_t$$

We first note that we must obtain a closed-form solution for c_t and l_t to obtain the optimal value of s_{t+1}. Indeed, since s_{t+1} is linear in $\mathcal{L}$, we would need to plug the closed-form solutions of c_t and l_t in the budget constraint.

Replacing the expression of λ_t in the two other equation yields:

$$c_t^{-\rho} \cdot z_t = \xi_t \cdot l_t^{\varphi} \iff \begin{cases} c_t = \left[\frac{\xi_t \cdot l_t^{\varphi}}{z_t}\right]^{-\frac{1}{\rho}} \\ l_t = \left[\frac{c_t^{-\rho} z_t \cdot}{\xi_t}\right]^{\frac{1}{\rho}} \end{cases} \tag{6}$$

And

$$c_t^{-\rho} = \beta \cdot \mathbb{E}\left[c_{t+1}^{-\rho} \cdot (1 + r_{t+1})\right] + \gamma_t \tag{7}$$

Assuming that the budget constraint binds, it becomes, as previously seen:

$$c_t + s_{t+1} = l_t \cdot z_t + s_t \cdot (1 + r_t) \iff c_t = l_t \cdot z_t + s_t \cdot (1 + r_t) - s_{t+1}$$

This leads to the following equation system:

$$\begin{cases} c_t = \left[\frac{\xi_t \cdot l_t^{\varphi}}{z_t}\right]^{-\frac{1}{\rho}} \\ c_t = l_t \cdot z_t + s_t \cdot (1 + r_t) - s_{t+1} \end{cases}$$

$$\iff$$

$$\left[\frac{\xi_t \cdot l_t^{\varphi}}{z_t}\right]^{-\frac{1}{\rho}} = l_t \cdot z_t + s_t \cdot (1 + r_t) - s_{t+1}$$

$$\iff$$

$$l_t^{-\frac{\varphi}{\rho}} \cdot \left(\frac{\xi_t}{z_t}\right)^{-\frac{1}{\rho}} = l_t \cdot z_t + s_t \cdot (1 + r_t) - s_{t+1}$$

$$\iff$$

$$l_t^{-\frac{\varphi}{\rho}} \cdot \left(\frac{z_t}{\xi_t}\right)^{\frac{1}{\rho}} - l_t \cdot z_t - s_t \cdot (1 + r_t) - s_{t+1} = 0$$

This is a transcendantal equation of form $x^{\alpha} \cdot b - x \cdot y - c = 0$, which admits a solution if and only if $-\frac{\varphi}{\rho} \in \mathbb{N}$. This condition seems unrealistic in our context:

- $-\varphi > 0$ implies that labor has a decreasing disutility, which makes the maximization program absurd.
- $-\rho > 0$ implies a risk-loving agent, which changes drastically the framework of our model, and would require another whole interpretation.

Note that if we set $-\rho \in \mathbb{N}$ and further develop the last equation in the budget constraint binding attempt, we end up with the same condition.

9.3.4 Backwards solving attempt

If we try to solve it backwards, we now go to the last period. At the last period, $s_{t+1} = \underline{s}$ for sure: Since there is no future, the agent will borrow as much as they can, or will at least not save anything more than what is imposed by the constraint.

For simplification, let $\underline{s}$ be fixed such that: $\underline{s} = 0$. The new optimality condition is:

$$l_t^{\varphi} \cdot \xi_t = [l_t \cdot z_t + s_t \cdot (1 + r_t)]^{-\rho} \cdot z_t \tag{8}$$

Although we simplified the term at the exponential of which we have $-\rho$, this is still a transcendantal equation due to the sum of labor income and income coming from savings of last period, and the problem remain the same.